Processing and properties of graded ceramic filters

Suelen Barg, Dietmar Koch, Georg Grathwohl

Angaben zur Veröffentlichung / Publication details:

Barg, Suelen, Dietmar Koch, and Georg Grathwohl. 2009. "Processing and properties of graded ceramic filters." *Journal of the American Ceramic Society* 92 (12): 2854–60. https://doi.org/10.1111/j.1551-2916.2009.03301.x.

Processing and Properties of Graded Ceramic Filters

Suelen Barg,† Dietmar Koch, and Georg Grathwohl

Ceramic Materials and Components, University of Bremen, D-28359 Bremen, Germany

A new processing route for high-performance graded ceramic filters is presented. The direct foaming process is based on the transition of a surfactant-stabilized alkane dispersion in a stabilized aqueous ceramic powder suspension into mechanically stable ceramic foams with porosities up to 90%. The cell size distribution and, consequently, the permeability of the filters could be efficiently adjusted by the control of the high alkane phase-emulsified suspension (HAPES) microstructure during emulsification. Furthermore, open porous graded structures are produced by combining HAPES layers with different droplet sizes. The tailored microstructural features, providing controlled permeabilities as well as high compressive strength of the cellular ceramics are of special interest for applications where fluid transport through ceramic microstructures is required. These include filters, in particular for aerosol filtration, temperature control membranes in autothermal reforming, catalytic supports including supports for batteries as well as matrices for immobilized microorganisms.

I. Introduction

Porous ceramics with controlled porosity parameters present a combination of advantageous properties such as high-temperature stability, good thermal insulation properties, low weight, as well as high-permeability and high-accessible surface area in the case of open porosity. Consequently, they are attractive materials for an increasing number of applications. These include molten metal, aerosol and hot gas filters, catalytic supports, supports for batteries and fuel cells, bioreactors, pore burners, and scaffolds for tissue engineering.[1–3]

The processing route has a decisive influence on the microstructural features, namely composition and porosity parameters, as well as on the final properties of the porous materials. The main processes available so far for the fabrication of macroporous ceramics have been described recently in handbooks and review papers.[1–3] The direct foaming techniques are of particular interest due to their simplicity, flexibility, and low cost. Recently, a versatile direct foaming method has been developed where an alkane phase is emulsified in an aqueous ceramic powder suspension, giving rise to cellular structures with controllable cell sizes from a few micrometers up to the millimeter scale.[4,5] Emulsions have also been used as templates for the determination of porosity parameters in inorganic porous structures.[6,7]

Functionally graded materials (FGM) have been developed with specific structural, compositional, morphological, and mechanical properties.[8] Porous ceramics exhibiting graded porous structures are a special type of FGM and are required for several applications. Graded porous ceramics with closed porosities are proposed, for example, as bulk thermal shock-resistant structures for high-temperature applications[9] as well as for thick thermal barrier coatings.[10] Applications of graded porous ceramics where open porosity is important include, for example, their use as preforms for liquid metal infiltration yielding functionally graded metal/ceramic composites.[11] This class of materials also shows potential for use as scaffolds for tissue engineering, where efforts are made for the design of porosity gradients mimicking the bone structure.[12,13] The use of graded open porous ceramics as double-layered aerosol filters is especially demanded, where the presence of a thin layer with smaller cell sizes provides a physical barrier associated with a minimum pressure loss due to the support layer with larger cell sizes.[14] Furthermore, their use as temperature control membranes for autothermal reforming (ATR) is also envisaged.[15]

Graded porous ceramics are usually produced by packing of powder or fibers at varying densities, followed by partial sintering.[16] They are also produced by an induced segregation of metastable suspensions,[17] controlled sintering of compacted ceramic and carbon powder mixtures,[16] and by electrochemical processing.[13] Furthermore, the lamination of green tapes with different porosity parameters achieved by the percolation of pyrolyzable particles,[11] the direct foaming of a pure silicone resin[18] as well as of a Si/SiC-filled silicone resin[19] are shown as possible processing routes for the realization of open porous graded ceramics with specific characteristics. Although considerable progress has been achieved in the processing of graded porous ceramics,[11,13,16–19] further requirements have to be envisaged when high interconnectivities of differently sized pores in a mechanically strong ceramic part have to be achieved.

In this work, mechanically stable alumina filters with a monomodal interconnected cell size distribution as well as with gradients of the cell size are produced via a layer-by-layer process in combination with a simple direct foaming process, based on the transition of a high alkane phase-emulsified suspension (HAPES) into cellular ceramics. The processing route can be adapted for many different compositions and systems, providing excellent mechanical properties due to the defect-free build-up of the struts and, particularly, tailored microstructural features as highly interconnected cells even between adjacent layers. In these systems, it is very important to control the alkane droplet size due to its strong influence on the rheological properties and stability of the emulsified suspensions, controlling finally the stereological parameters of the emerging ceramic foams. Recently, it has been shown in more detail that the droplet size distribution in HAPES can be efficiently controlled by adjusting the parameters of stirring rate during the emulsification process and the particle content of the alumina suspensions.[5] Therefore, the objectives of this work are to develop alumina filters with varying cell sizes as provided by controlled mechanical shearing during the HAPES emulsification. The processing route to be developed then yields to graded structures with open porosity throughout the adjacent layers of the filters.

II. Experimental Procedure

(1) Filter Preparation

For the production of the filters, HAPES is prepared. The first step is the preparation of a stabilized alumina powder suspension. A dry alumina powder (Alcoa CT 3000 SG, Alcoa, Frankfurt, Germany) with an average particle diameter (d_{50})

T. Ohj—contributing editor

†Author to whom correspondence should be addressed. e-mail: sbarg@uni-bremen.de

of 500 nm and a specific surface area of 7.5 m^2/g is slowly added to deionized water containing Dolapix CE–64 (0.74 wt% related to alumina) as a negatively charged electrosteric dispersion agent under severe mixing. Dispersion and homogenization is carried out in a laboratory mixer (Dispermat LC, VMA Getzmann GmbH, Reichshof, Germany) at a mixing velocity of 2500 rpm for 20 min. The particle content in the suspensions is set at 42 vol%. Afterwards, the suspensions are subjected to deaeration to remove undesired entrapped bubbles under reduced pressure (5 kPa).

HAPES is then prepared by adding 70 vol% decane from Fluka (Steinheim, Germany) and sodium lauryl sulfate (BASF, Lutensid AS 2230, BTC, Köln, Germany) as an anionic surfactant (between 0.11 and 0.22 vol%, depending on the stirring rate used). To ensure the stability of the system, the addition of this surfactant has to take into account the ξ potential and the isoelectric point of the alumina suspension. Therefore, it is used under alkaline conditions (pH 9.5), where a strong negative ξ potential is provided by the dispersion agent.[4]

The droplet size during emulsification is controlled by the application of different stirring rates (from 800 to 2500 rpm) for 2.5 min. The suspensions are emulsified under reduced pressure (10 kPa) at room temperature to avoid abundant incorporation of air bubbles; this pressure is not reduced further because evaporation of decane, which has a vapor pressure of 0.19 kPa at 25°C, may be hindered.

The methodology used for the production of the materials consists in casting the HAPES of a defined composition into a stationary PVC mold (90 mm × 42 mm and 90 mm × 70 mm with variable height). A doctor blade is then moved along the surface of the filled mold, which ensures the removal of excess HAPES and provides precise shaping of the green foam keeping the upper surface open to the atmosphere. This procedure can be applied repeatedly after elevating or replacing the original mold wall segments by slightly higher components. A second casting step follows and if the secondary HAPES differs in its emulsification parameters from the first one, a change in the cell size between the first and the second layer is achieved. As the interface between the layers can be a main problem for the realization of graded structures, the doctor blade can be moved again after a defined time along the surface to remove the dried upper film of the previous layer, ensuring, therefore, a perfect coupling and an open porous interface between the adjacent layers.

The consolidation of the molded HAPES proceeds under limited foaming by a minimal expansion of the alkane droplets and drying of the aqueous solvent. Complete drying of the foams is achieved at room temperature during 3 days. After demolding, the shaped green alumina filters are sintered at 1550°C for 2 h at heating and cooling rates of 2 K/min.

(2) Filter Characterization

The morphology and microstructure of the sintered materials are evaluated by scanning electron microscopy (Camscan 24, Cambridge, U.K.). Cell sizes are measured from planar sections with the linear intercept method using the software Linear Intercept (TU Darmstadt). The average cell size d_{50} is determined from the cumulative cell size distribution curves of three pictures taken from different regions of the sample. The total and open porosity of the materials is calculated using the Archimedes method considering three different weights of the specimen: m_1 (the dry specimen weight), m_2 (weight of the specimen under water), and m_3 (weight of the wet specimen). The window size distribution is measured by Hg-Intrusion (Pascal 140/440, CE Instruments, Hofheim/Ts., Germany).

The permeability is measured using a professional tool (Topas PSM 165, Dresden, Germany) where the gas mass flow rate through the materials is measured for controlled differential pressures ranging from 0 to 1 bar. Forchheimer's equation (Eq. (1)) is expressed as a parabolic relationship between pressure drop (Δp) and the superficial velocity of the fluid (u). The permeability coefficients K_1 and K_2 are calculated by Forchheimer's equation expressed for flow of compressible fluids fitting the experimental data by a standard least squares method.[20]

$$\frac{\Delta p}{l} = \frac{\mu}{K_1}u + \frac{\rho}{K_2}u^2 \quad \text{with } \Delta p = \frac{p_i^2 - p_0^2}{2p_0} \tag{1}$$

where p_i and p_0 denote, respectively, the pressure of incoming gas flow before and after passing through the filter, l is the filter thickness (2.4–3.8 mm), ρ is the gas density (1.19 kg/m^3), and μ the gas viscosity ($1{,}83 \times 10^{-5}$ Pa · s), which are calculated for reference conditions of $p_0 = 1010$ mbar and room temperature. The superficial velocity of the fluid ($u = V/A$) is calculated from the volumetric flow rate V at the above-mentioned reference conditions, considering an effective free flow area A of 0.95 cm^2. Uniaxial compressive strength tests are performed in a hydraulic mechanical testing machine (Zwick Model, Ulm, Germany), following the ASTM C133-94 standard. The crosshead speed is 1.3 mm/min and a compressive load cell of 5000 N is used. For each parameter investigated, 20–30 specimens measuring 10 mm × 10 mm × 10 mm in size are cut from a ceramic part (90 mm × 70 mm × 15 mm) with a diamond disk and ground to ensure parallel surfaces. The compressive strengths are calculated from the maximal stress in the compressive stress–strain curves.

III. Results and Discussion

(1) Processing of Filters with Designable Microstructures

It is very important to control the alkane droplet size distribution for the realization of stable green bodies and, consequently, cellular ceramics with defined porosity parameters. The transition of HAPES to stable green bodies is achieved upon evaporation of the solvents with a minimal expansion of the pore formers. This simple and versatile process yields strong ceramic foams in which the desired porosity parameters can mainly be controlled by the adjustment of droplet size and density during the emulsification process.

Filters resulting from sintering (1550°C/2 h) of stable green bodies are shown in Fig. 1. The filters based on HAPES composed of 70 vol% decane and processed by the methodology described in "Filter Preparation" undergo 12%–14% linear shrinkage during sintering. Microstructures of monolayered filters produced from HAPES emulsified under 800, 1500, and 2500 rpm are represented in Fig. 2. The materials are characterized by highly interconnected cells, uniformly distributed throughout the sample. The emulsification stirring rate controls the droplet size and, consequently, the cell size distribution, which will be quantified below. In spite of the strongly varying microstructure, the total porosity was efficiently maintained between 77.6% and 78.8% by maintaining the HAPES alkane content constant (Fig. 3). The highly interconnected cells yield as high open porosities. Furthermore, increase of the emulsification stirring rate beyond 1100 rpm yields to completely opened porosities.

As a consequence of the fixed total porosity, smaller cell-sized structures present a higher concentration of cells and a higher specific surface area is thus obtained. However, the number of connections between cells is high and approximately the same for larger as well as for smaller cell-sized structures (Fig. 2). Consequently, larger cell sizes and lower specific surface areas develop into thicker struts. Besides the struts or cell edges, the microstructure consists of cell faces in the form of thin films (lamellae), which connect two alkane droplets in HAPES and the bubbles emerging from this phase. During evaporation and drying, these bubbles open up partially, thereby providing windows between adjacent cells. The windows size is proportional to the cell size and decreases like the cell size with an increasing stirring rate.

The quantitative results providing average sizes of cells, windows, and struts are presented in Fig. 4 as being influenced by

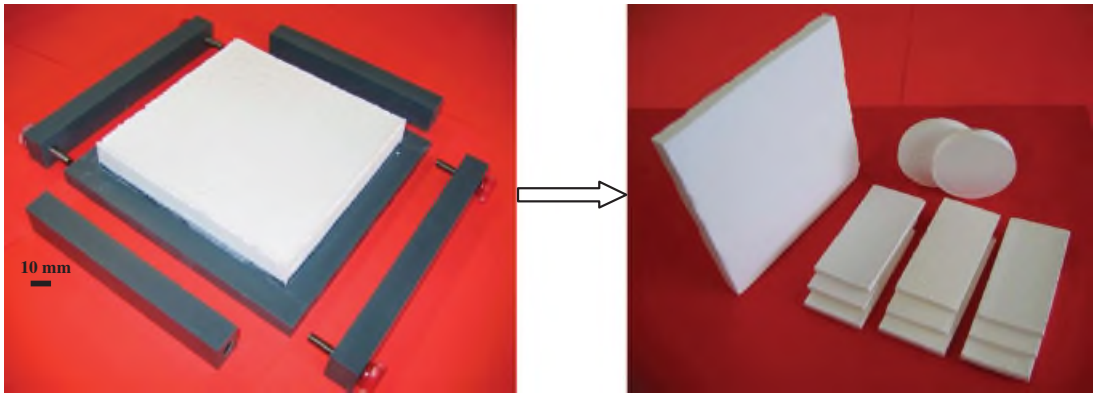

Fig. 1. Stable demolded green body (left) and resulting sintered (1550°C/2 h) alumina filters (right). The filters with controlled microstructural features are based on high alkane phase-emulsified suspension composed of 70 vol% decane emulsified in the powder suspension (solids fraction 42 vol%).

the stirring rate. A reduction of the average cell size (d_{50}) from 20 to 6 μm, the average window size from 13 to 4 μm, and the strut thickness from 14 to 3 μm is measured when HAPES is emulsified under 800 and 2500 rpm, respectively. The cumulative cell size distributions of the corresponding ceramic foams are depicted in Fig. 5. The broad cell size distribution (with d_{10} and d_{90} of 7 and 48 μm, respectively) obtained by emulsification under 800 rpm is strongly reduced by higher stirring rates. Uniform microstructures with a narrow cell size distribution presenting d_{10} and d_{90} of 3 and 11 μm, respectively, are obtained by emulsification under 2500 rpm. Large cell-size distributions (resulting from emulsification under 800 and 1100 rpm) may occasionally yield isolated small pores enclosed in the struts (Fig. 2), resulting in some reduction of open porosity (Fig. 3). In this way, the microstructure of monolayered filters could be efficiently designed by controlling the shear stresses in the droplets' surface during emulsification. The potential to produce crack-free, open porous ceramic filters with controllable porosity parameters is a manifestation of the high structural stability of HAPES, which resists capillary stresses during consolidation, with a minimum expansion of the pore formers.

(A) Graded Filters: Given the stability and advantages of this direct foaming process, open porous graded structures with coupling interfaces are produced by the combination of layers composed of HAPES with different droplet sizes. A bilayer filter is presented in Fig. 6, as it is prepared under fixed chemical conditions by varying the stirring rate for emulsification. While the porosity is constant in all sections of the sample, the average cell size increases from top to bottom due to the reduced stirring rate. In particular, the interface between the layers with small and large sizes of the cells and windows provides a defect-free transition between the lower and the upper part of the sample. The intermediate state is in fact characterized by a large cell size (typical for the lower part), which contains a high

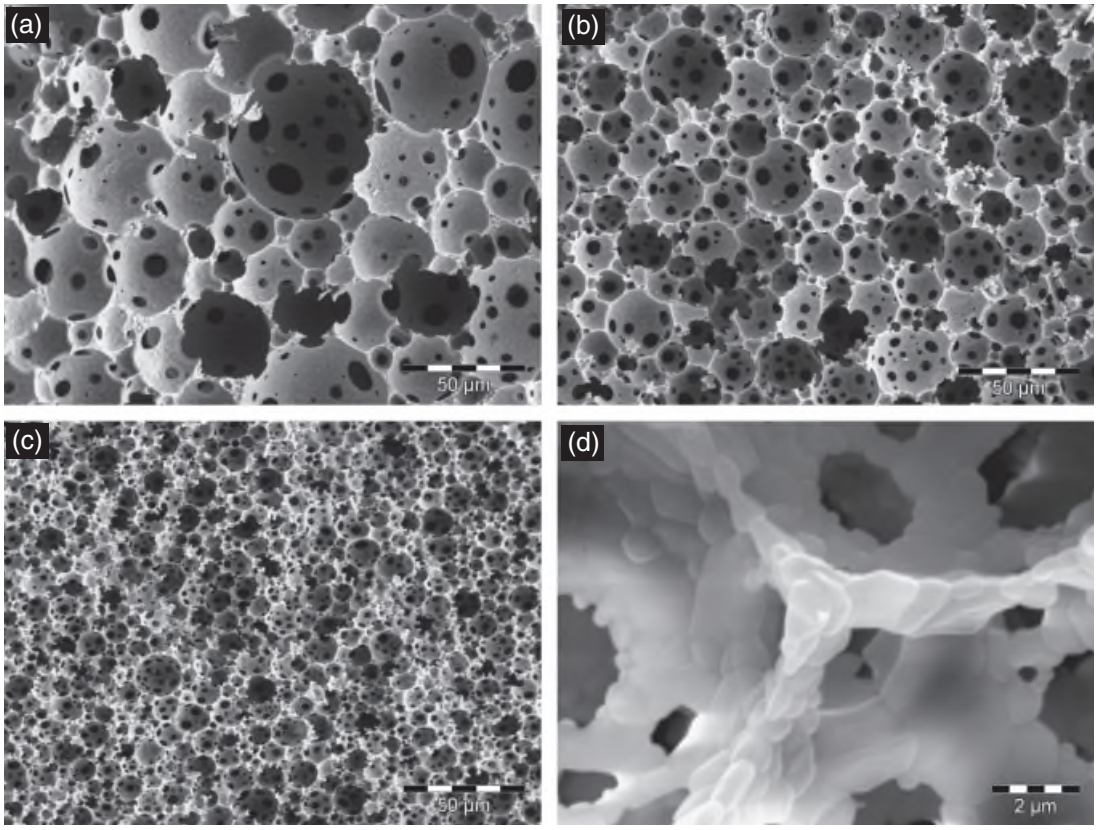

Fig. 2. Microstructure of sintered alumina foams produced from high alkane phase-emulsified suspension emulsified under the stirring rates (a) 800 rpm, (b) 1500 rpm, (c) and (d) 2500 rpm of the powder suspension (solid fraction 42 vol%). Dense struts constituted by a monolayer of alumina particles are represented in (d).

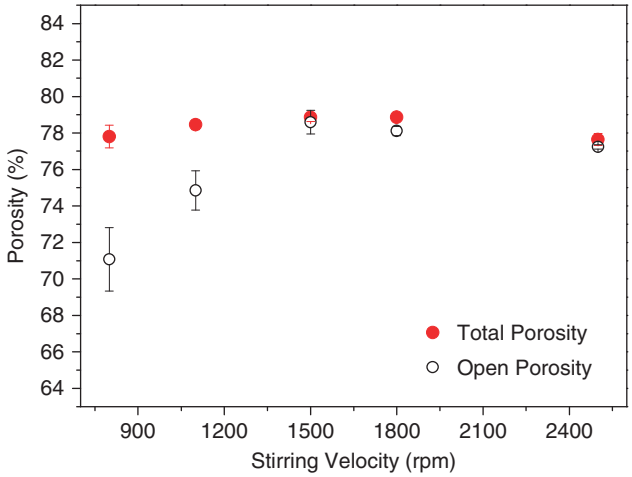

Fig. 3. Total and open porosity of alumina cellular ceramics emulsified under increasing stirring rates.

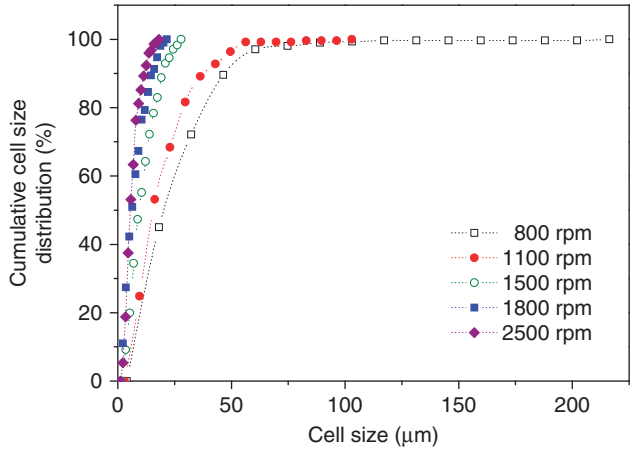

Fig. 5. Cumulative cell size distribution of alumina filters as a function of the emulsification stirring velocity.

number of small windows being characterized by the upper part. The constituting elements of both parts are then simultaneously present on the interface.

The successful realization of gradients with interconnecting interfaces has to take into account the time of successive casting and the viscosity of the subsequent layer. In this way, previous layers should be thicker or should have higher viscosities in order to prevent mixing with the subsequent layer. In addition, the time interval between both casting steps should be sufficient to promote some consolidation of the previous layer. In some cases, the doctor blade can be moved again over the surface to remove the dried surface film of the previous layer, thereby ensuring a coupled and open porous interface. By adjusting these parameters, multilayered open porous filters can be constructed from HAPES with gradients in cell and window sizes.

(2) Filter Properties

The permeability of porous materials is influenced by the porosity parameters and the processing route. Experimental flow curves for the determination of the permeability coefficients, K_1 and K_2, are shown in Fig. 7. The curves present a parabolic trend that is confirmed by the excellent fitting of Forchheimer's equation. However, the quadratic term ($\rho u^2/K_2$) is less pronounced in comparison with the linear term ($\mu u/K_2$), confirming the higher reliability of K_1 values.

The filters' permeability constants K_1 and K_2, as a function of the emulsification stirring rate, are represented in Fig. 8. Comparing Figs. 4 and 8, it can be concluded that with the decrease of the cell and window size, the permeability also decreases. The filters with controlled cell structures yield permeability constants varying between 3.8×10^{-12} and 3.9×10^{-13} m^2 for K_1 and 2.3×10^{-6} and 2×10^{-7} m for K_2. Recently, Innocentini *et al.*[21] have shown a numerical relationship between K_1 and K_2 that fits a large number of porous materials from concretes and bricks to replica foams. The filters produced in this work present permeability values that match the group of gel cast foams, fibrous, and granular filters used for aerosol filtration (especially for hot cleaning). Cell size and permeability of the developed cellular ceramics point them as potential candidates for their use as aerosol filters (K_1 in the range of 10^{-12} m^2)[14,22,23] as well as temperature control membranes in ATR (K_1 in the range of 10^{-12}–10^{-13} m^2)[15].

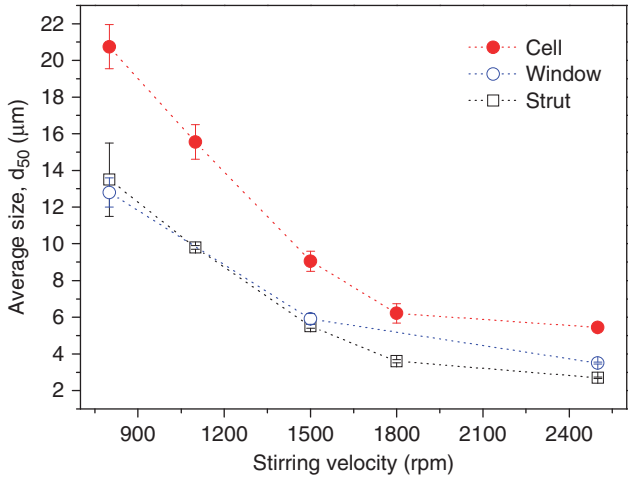

Fig. 4. Average cell, window, and strut size (d_{50}) of sintered alumina filters as a function of the emulsification stirring velocity.

The compressive strength of the alumina foams is correlated with the microstructural features, as proposed by Gibson and Ashby[24]:

$$\frac{\sigma_{cr}}{\sigma_{fs}} = C_6\left(\phi\left(\frac{t}{l}\right)^2\right)^{3/2} + (1+\phi)\left(\frac{t}{l}\right)^2 \qquad (2)$$

where σ_{cr} is the crushing strength, σ_{fs} the modulus of rupture of the cell-wall material (400 MPa),[25] C_6 is a constant (0.2), t is the strut thickness, l is the cell size, and ϕ is the fraction of solid contained in the cell edges. The remaining fraction ($1-\phi$) is the material present in the cell faces. Larger cell sizes with a lower surface area yield structures composed of thicker struts (shown in Fig. 4). The average strut thickness (t_{50}) as well as the strut thickness to cell size ratio (t_{50}/l_{50}) as a function of the average cell size (l_{50}) are plotted in Fig. 9. The strut thickness increases linearly with the cell size ($t = 0.69l$–0.85), resulting in a rational increase of $t/l = -0.85/l + 0.69$. A limiting value of $t/l = 0.69$ is then obtained for large cells.

The compressive strength of alumina foams as a function of t_{50}/l_{50} and its correlation with Eq. (2) are plotted in Fig. 10. As proposed by Gibson and Ashby, the compressive strength tends to increase with the increasing t/l (Fig. 10). However, alumina foams with the highest t/l (produced under the lowest stirring rate of 800 rpm) presented a lower compressive strength (29.5 MPa) than expected, which may be the effect of the broad cell size distribution and the presence of closed pores inside the struts.

While the total porosity of all investigated filters is fixed at the level of 78%, the cell sizes are varied considerably. The number of connections between adjacent cells is, however, nearly constant and the window size is proportional to the cell size. The fraction of material contained in the cell edges ϕ is then efficiently also maintained constant. The experimental strength

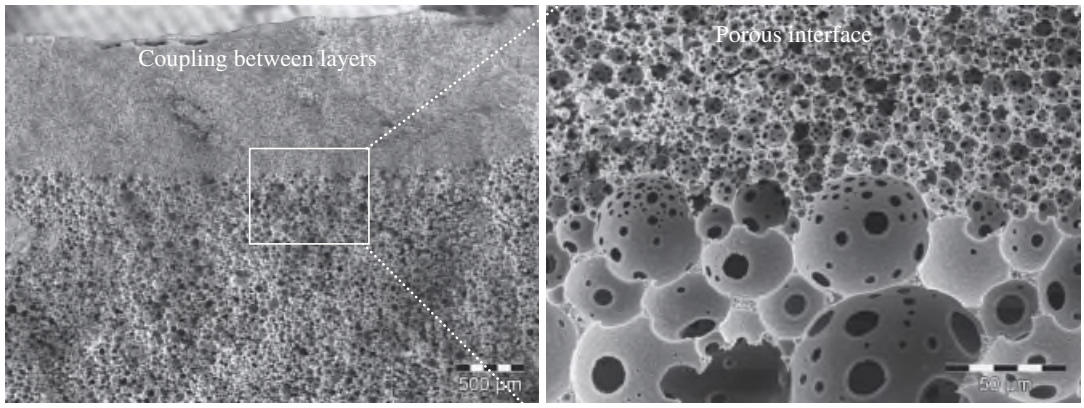

Fig. 6. Open porous graded filter produced from high alkane phase-emulsified suspension emulsified under 800 rpm (bottom layer—7 mm thick) and 2500 rpm (top layer—1 mm thick). The optimum delay time for the casting of the top layer in this system is 15 min.

data are then fitted, confirming a constant parameter $\phi = 0.9$ by Eq. (2). The experimental and fitted data are presented with their dependence on the strut thickness to cell size ratio in Fig. 10; the borderlines describing the relationship of Eq. (2) for $\phi = 0$ and 1 are also shown.

In summary, the processing route based on HAPES yields highly open porous ceramic materials (open porosity between 71% and 78%, total porosity of 78%, $\phi = 0.9$) with predetermined microstructures and excellent compressive strengths from 17.3 to 33.6 Mpa, depending on the t/l ratio.

The reported compressive strength data are compared with potential alumina aerosol filters (total porosity between 62% and 73%, open porosities up to 60%) fabricated by more conventional methods. The direct foaming process yields compressive strengths between 1.8 and 3.2 MPa.[26] Open porous alumina foams produced from particle-stabilized emulsions (total porosity of 72%) yielded a compressive strength of 13 MPa.[7] In a recent review, alumina porous structures with total porosities close to 80% produced via direct foaming are reported to yield compressive strength values up to 30 MPa.[2] However, in these cases, the degree of open porosity and the ratio of strut thickness to cell size are not reported.

(3) Graded Filters

The best performance of filters can be achieved by the realization of graded structures with combined microstructural features. Crack-free graded filters with 79% porosity are produced by the combination of a bottom layer emulsified under 800 rpm and a top layer emulsified under 2500 rpm, resulting in increasing cell sizes of 21 and 5 µm, respectively (Fig. 6). If we neglect the effects of the interface between layers (composed of large cells and small windows), the total pressure loss of the graded filters can be estimated by the sum of pressure loss correspondent to each layer. Considering ρ and µ (from Eq. (1)) as constant in all cases, the permeability coefficients K_{g1} and K_{g2} for a graded filter with total thickness l can be calculated as

$$K_{g1} = \frac{l}{\left(\frac{l_1}{K_{11}} + \frac{l_2}{K_{12}}\right)} \tag{3}$$

$$K_{g2} = \frac{l}{\left(\frac{l_1}{K_{21}} + \frac{l_2}{K_{22}}\right)} \tag{4}$$

where l_1, K_{11}, K_{21} and l_2, K_{12}, K_{22} represent the thickness and permeability constants of layers 1 and 2, respectively.

Based on this assumption, the combination of the bottom layer ($l_1 = 3.2$ mm, $K_{11} = 3.8 \times 10^{-12}$ m^2, $K_{21} = 2.3 \times 10^{-6}$ m) composed of large cell sizes with the top layer ($l_2 = 0.6$ mm, $K_{12} = 3.9 \times 10^{-13}$ m^2, $K_{22} = 2.0 \times 10^{-7}$ m) composed of smaller cell sizes results in graded filters with permeability values of $K_{g1} = 1.4 \times 10^{-12}$ m^2 and $K_{g2} = 7.6 \times 10^{-7}$ m. The experimentally determined permeability constants are measured as $K_{g1} = 1.42 \times 10^{-12}$ m^2 and $K_{g2} = 1.2 \times 10^{-6}$ m, which are in reasonable agreement with the values expected from Eqs.(3) and (4). A few small differences between measured and predicted permeabilities can be attributed to the effect of the interface between layers, which is composed of a combination of large cells

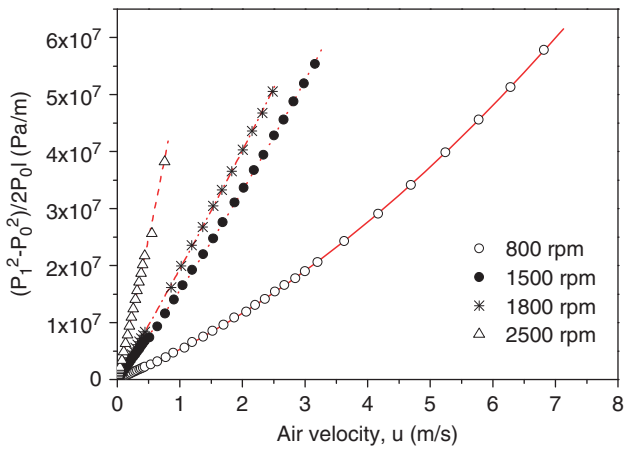

Fig. 7. Typical pressure drop curves obtained for the alumina filters emulsified under varying stirring rates.

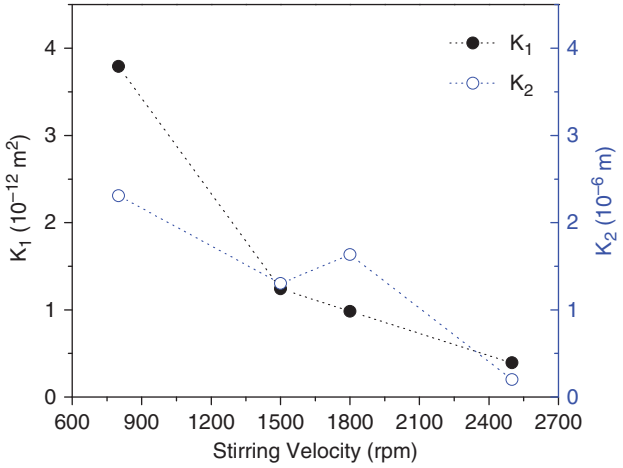

Fig. 8. Alumina filters permeability constants K_1 and K_2 (see Eq. (1)) as a function of the emulsification rate. Open and total porosities as well as cell and window sizes are indicated in Figs. 3 and 4.

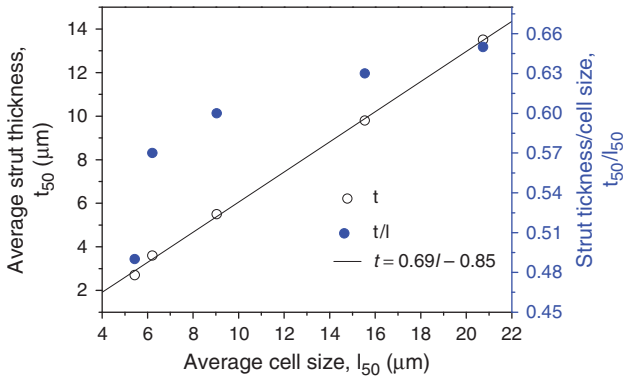

Fig. 9. Strut thickness and strut thickness to cell size ratio as a function of cell size.

and small windows. It should be emphasized, however, that considerabe benefit is realized by the graded filter combining the filtering capacity of the small cell-sized layer with a permeability approaching the higher level of the large-sized layer. Furthermore, the graded materials present high compressive strength averaging in (24.3 MPa), which is higher than in the case of monolayered small-sized filters emulsified under 2500 rpm (17.3 MPa).

The adjustment of the top layer thickness as well as the application of subsequent layers can be used to design these materials for fast particulate deposition and high filtration efficiency, associated with adjusted pressure drop combining, therefore, in one product the advantageous features of both fibrous and granular filters.[14] Furthermore, adjustment of varying permeabilities due to a graded structure can be applied to control the O_2 supply in methane autothermal reformers maintaining, therefore, a constant temperature during H_2 production, which yields, in addition to other advantages, an increase of the components' durability.[15]

IV. Conclusions

With the processing route based on the transition of HAPES into cellular ceramics, it is possible to realize graded as well as monomodal filters composed of highly interconnected structures. The cell size distributions can be controlled by the stirring rate during the emulsification process, from larger cells (21 µm) with broad cell size distributions to smaller cells (5 µm) with very narrow cell size distributions resulting in permeabilities appropriate for filtering applications.[14]

The possibility in controlling the microstructural features, namely, the ratio of strut thickness to cell size (t/l) by keeping other parameters like the fraction of materials in the cell edges (ϕ) as well as the total porosity constant, makes the properties of the filters adjustable for application requirements. Corresponding with this microstructural control, the open porous materials presenting a very high compressive strength can be interpreted by the microstructural correlations proposed by Gibson and Ashby.[24]

Furthermore, crack-free gradient filters composed of layers with different combinations of cell sizes (5 and 21 µm) could be produced, yielding remarkable compressive strength (24.3 MPa), and permeabilities in the range of $K_1 = 1.42 \times 10^{-12}$ m^2 and $K_2 = 1.2 \times 10^{-6}$ m. The transition from the large-to small-sized cells and windows is accomplished by a defect-free self-assembled intermediate stage composed of large cells and small windows.

The advantages of this processing route can be found particularly in the efficient control of microstructural features and consequently properties, excellent compressive strengths as well as the possibility of forming layers of stable emulsions leading to graded structures of self-assembled open porous interfaces. These materials can then be used in several applications where fluid transport through ceramic microstructures is required. The use of gradient structures as double-layered filters as well as ATR temperature control membranes is especially envisaged.

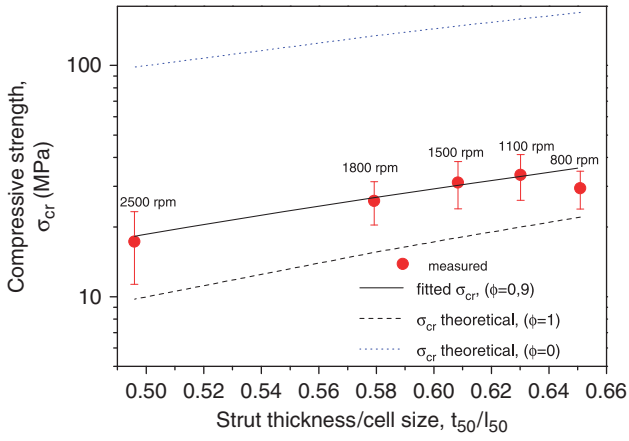

Fig. 10. Compressive strength as a function of strut thickness to cell size ratio for different stirring velocities. The broken borderlines represent the compressive strength expected for closed ($\phi = 0$) and open cell foams ($\phi = 1$), according to the theoretical model of Gibson and Ashby. The solid line describes the compressive strengths of the studied alumina filters ($\phi = 0.9$); open and total porosities are indicated in Fig. 3.

Acknowledgments

The authors would like to thank DFG for funding this project within the Research Training Group 1375 "Nonmetallic Porous Structures for Physical-Chemical Functions." The contributions of Jens Hüppmeier and Nicolas Fries for the permeability measurements at ZARM (University of Bremen) and of the students Elisângela G. de Moraes, Lígia Barbosa, Mateus Carlesso, and Hailing Wang for their help in the experimental work are gratefully acknowledged.

References

[1]M. Scheffler and P. Colombo, *Cellular Ceramics: Structure, Manufacturing, Properties and Applications*. Wiley-VCH, Weinheim, 2005.

[2]A. R. Studart, U. T. Gonzenbach, E. Tervoort, and L. J. Gauckler, "Processing Routes to Macroporous Ceramics: A Review," *J. Am. Ceram. Soc.*, **89** [6] 1771–89 (2006).

[3]P. Colombo, "Conventional and Novel Processing Methods for Cellular Ceramics," *Philos. Trans. R. Soc.-Math. Phy. Eng. Sci.*, **364** [1838] 109–24 (2006).

[4]S. Barg, C. Soltmann, M. Andrade, D. Koch, and G. Grathwohl, "Cellular Ceramics by Direct Foaming of Emulsified Ceramic Powder Suspensions," *J. Am. Ceram. Soc.*, **91** [9] 2823–9 (2008).

[5]S. Barg, E. G. Moraes, D. Koch, and G. Grathwohl, "New Cellular Ceramics from High Alkane Phase Emulsified Suspensions (HAPES)," *J. Eur. Ceram. Soc.*, **29** [12] 2439–46 (2009).

[6]A. Imhof and D. J. Pine, "Ordered Macroporous Materials by Emulsion Templating," *Nature*, **389** [6654] 948–51 (1997).

[7]I. Akartuna, A. R. Studart, E. Tervoort, and L. J. Gauckler, "Macroporous Ceramics from Particle-Stabilized Emulsions," *Adv. Mater.*, **20** [24] 4714–8 (2008).

[8]S. Suresh and A. Mortensen, *Fundamentals of Functionally Graded Materials*. The Institute of Materials, London, 1998.

[9]J. P. S. K. Satyamurthy, M. P. Kamat, and D. P. H. Hasselman, "Effect of Spatially Varying Porosity on Magnitude of Thermal Stress During Steady-State Heat Flow," *J. Am. Ceram. Soc.*, **62** [7–8] 431–2 (1979).

[10]H. Steffens, Z. Babiak, and M. Gramlich, "Some Aspects of Thick Thermal Barrier Coating Lifetime Prolongation," *J. Therm. Spray Technol.*, **8** [4] 517–22 (1999).

[11]S. F. Corbin, X. Zhao-jie, H. Henein, and P. S. Apte, "Functionally Graded metal/Ceramic Composites by Tape Casting, Lamination and Infiltration," *Mater. Sci. Eng. A*, **262**, 192–203 (1999).

[12]A. Tampieri, G. Celotti, S. Sprio, A. Delcogliano, and S. Franzese, "Porosity-Graded Hydroxyapatite Ceramics to Replace Natural Bone," *Biomaterials*, **22**, 1365–70 (2001).

[13]J. P. Werner, C. Lathe, and P. Greil, "Pore-Graded Hydroxyapatite Materials for Implantation," *Br. Ceram. Proc.*, **60** [2] 547–8 (1999).

[14]N. L. de Freitas, J. A. S. Goncalves, M. D. M. Innocentini, and J. R. Coury, "Development of a Double-Layered Ceramic Filter for Aerosol Filtration at High-Temperatures: The Filter Collection Efficiency," *J. Hazard. Mater.*, **136** [3] 747–56 (2006).

[15]J. Huppmeier, M. Baune, and J. Thoeming, "Interactions Between Reaction Kinetics in ATR-Reactors and Transport Mechanisms in Functional Ceramic Membranes: A simulation Approach," *Chem. Eng. J.*, **142** [3] 225–38 (2008).

[16]K. Maca, P. Dobsak, and A. R. Boccaccini, "Fabrication of Graded Porous Ceramics Using Alumina–Carbon Powder Mixtures," *Ceram. Int.*, **27** [5] 577–84 (2001).
[17]K. Darcovich and C. R. Cloutier, "Processing of Functionally Gradient Ceramic Membrane Substrates for Enhanced Porosity," *J. Am. Ceram. Soc.*, **82** [8] 2073–9 (1999).
[18]P. Colombo and J. R. Hellmann, "Ceramic Foams from Preceramic Polymers," *Mater. Res. Innov.*, **6** [5–6] 260–72 (2002).
[19]J. Zeschky, T. Hofner, C. Arnold, R. Weissmann, D. Bahloul-Hourlier, M. Scheffler, and P. Greil, "Polysilsesquioxane Derived Ceramic Foams with Gradient Porosity," *Acta Mater.*, **53** [4] 927–37 (2005).
[20]W. Acchar, E. G. Ramalho, F. B. M. Souza, W. L. Torquato, V. P. Rodrigues, and M. D. M. Innocentini, "Characterization of Cellular Ceramics for High-Temperature Applications," *J. Mater. Sci.*, **43**, 6556–61 (2008).
[21]M. D. M. Innocentini, P. Sepulveda, and F. S. Ortega; pp. 313–4 in *Cellular Ceramics: Structure, Manufacturing, Properties and Applications*, Edited by M. Scheafler, and P. Colombo. Wiley-VCH, Weinheim, 2005.
[22]K. Darcovich, K. A. Jonasson, and C. E. Capes, "Developments in the Control of Fine Particulate Air Emissions," *Adv. Powder Technol.*, **8** [3] 179–215 (1997).
[23]K. Sutherland, *Filters and Filtration Handbook*, 5th edition, Elsevier, Oxford, UK, 2008.
[24]L. J. Gibson and M. F. Ashby, *Cellular Solids: Structure & Properties*. Cambridge University Press, Cambridge, UK, 1997.
[25]S. Saito, *Fine Ceramics*. Elsevier, New York, 1985.
[26]M. D. M. Innocentini, V. P. Rodrigues, R. C. O. Romano, R. G. Pileggi, G. M. C. Silva, and J. R. Coury, "Permeability Optimization and Performance Evaluation of Hot Aerosol Filters made Using Foam Incorporated Alumina Suspension," *J. Hazard. Mater.*, **162** [1] 212–21 (2009). □